Quantification of Saharan and local dust impact in an arid Mediterranean area by the positive matrix factorization (PMF)

Atmospheric Environment 42 (2008) 8872–8882

Contents lists available at ScienceDirect

Atmospheric Environment

journal homepage: www.elsevier.com/locate/atmosenv

Quantification of Saharan and local dust impact in an arid Mediterranean area by the positive matrix factorization (PMF) technique

Jose Nicolás [a,*], Massimo Chiari [b], Javier Crespo [a], Isabel Garcia Orellana [c], Franco Lucarelli [b], Silvia Nava [b], Carlos Pastor [a], Eduardo Yubero [a]

[a] Laboratory of Atmospheric Pollution (LCA), Miguel Hernández University, Av. de la Universidad s/n, Edif. Alcudia, 03202, Elche, Spain
[b] Physics Department, University of Florence and INFN, via Sansone 1, I-50019 Sesto Fiorentino, Italy
[c] Centro Nacional de Aceleradores (Seville University-CSIC-JA), Av. Thomas A. Edison, 7. 41092 Seville, Spain

ARTICLE INFO

Article history:
Received 3 December 2007
Received in revised form 23 July 2008
Accepted 4 September 2008

Keywords:
Atmospheric aerosol
Saharan dust
PM_{10}
PIXE
PMF

ABSTRACT

Particle composition data for PM_{10} samples collected at an urban background location in Elche in southeastern Spain from December 2004 to November 2005 were analysed to provide source identification and apportionment. A total of 120 samples were collected and analysed by Particle Induced X-ray Emission (PIXE) and ion chromatography. Positive matrix factorization (PMF) was used to estimate sources profiles and their mass contributions. The PMF modelling identified six sources: PM_{10} mass was apportioned to secondary nitrate (26%), secondary sulphate (22%), local soil dust (21%), traffic (13%), seasalt (11%) and African dust (7%). It is worth noting that PMF was able to identify a Saharan dust source even in the presence of a weighty local dust source, and to quantitatively estimate the contributions of these two sources. The African dust contribution varies, depending on the intrusion days, within a range of 5–40% of the total PM_{10} concentration. Without the contribution of Saharan dust, 50% of the total exceedances of the PM_{10} 50 $\mu g\,m^{-3}$ EC limit during the studied period would not have taken place.

1. Introduction

The use of statistical methodologies in multivariate analysis, like Principal Components Analysis (PCA) (Henry and Hidy, 1979), Cluster Analysis (CA) (Sánchez Gómez and Ramos Martín, 1987) or, of more recent application, Positive Matrix Factorization (PMF) (Paatero, 1997), is common in the identification of sources of atmospheric particulate matter (PM). However, it is difficult to discriminate contributions of long-range PM transport, even with the use of these techniques, because they are frequently masked by local sources, especially in urban environments.

Indeed, this could be the case in the distinction of crustal material sources. In this case, the mineral matter could have two different origins: local resuspension at the sampling site and the contribution of dust transported from areas like the Sahel region and Sahara Desert.

There is no doubt about the substantial contribution to Europe of cross-border crustal material coming from northern Africa, which annually is between 80 and 120 million tons (D'Almeida, 1986). The record of its arrivals, effects and characteristics in the continent has been extensively analysed in many areas: in the eastern Mediterranean (Kubilay et al., 2000), continental Europe (Schwikowski et al., 1995), the British Isles (Ryall et al., 2002), and western Mediterranean (Guerzoni et al., 1997; Ávila et al., 1997; Rodríguez et al., 2001).

Different techniques were utilised to identify the arrivals of these outbreaks to help confirming the origins of the PM level increases or possible variations in their chemical composition. The use of models, images and satellite data, reinforced with back-trajectory calculations

* Corresponding author. Tel./fax: +34 966658325.
E-mail address: j.nicolas@umh.es (J. Nicolás).

1352-2310/$ – see front matter © 2008 Elsevier Ltd. All rights reserved.
doi:10.1016/j.atmosenv.2008.09.018

(Dulac et al., 1992), has been complemented with the study of typical markers like the ratios of some crustal elements, for example Ti/Ca and Ti/Fe (Bonelli et al., 1996; Marenco et al., 2006; Borbély-Kiss et al., 2004). Another possibility for the study of long-range transport is the use of concentration fields (CF), a technique that combines information from back-trajectories with the PM component concentrations at the sampling site (Salvador et al., 2007).

Contributions from this crustal material primarily affect the coarse PM fraction. Under these events the crustal load in urban environments has reached up to 67% of the total PM_{10} mass contribution (Artiñano et al., 2003). It has to be noted that during these events, and due to the possible absorption of acidic gases like SO_2 or HNO_3 by mineral dust, high levels of non-marine sulphate and nitrate were recorded (Koçak et al., 2004).

Therefore, given the importance and frequency of this type of contributions, above all in geographic areas close to the northern half of the African continent, the purpose of this study is to quantify, by means of the PMF multivariate technique, the impact at ground level of crustal material transported by Saharan intrusions to PM_{10} concentration and to distinguish this contribution from that of local soil resuspension. This issue is particularly important and difficult in zones where a strong local soil contribution is present.

Moreover, the determination of the impact of Saharan dust provides the possibility of subtracting this contribution from the daily PM_{10} mass concentration on days when it exceeds the 50 $\mu g\,m^{-3}$ limit value fixed by EU Directive 2008/50/CE (it must not be exceeded more than 35 days per year). In this way, it is possible to determine the number of exceedances which are not due to the Saharan contribution. This information is important because the Directive specifies that the limits are not to be applied to events defined as natural (volcanic eruptions, geothermal and seismic activities, resuspension of particles, long-range transport from arid zones, etc.).

This methodology can either complement or be an alternative to the actual procedure admitted by the European Commission to discard natural exceedances from the annual calculation.

2. The studied area

PM_{10} concentration and composition was studied in the urban area of Elche (38°16′N; 0°41.5′W), a city with ~225,000 inhabitants in southeast Spain, located ~10 km from the Mediterranean coast. Its proximity to the African continent makes the area highly sensitive to dust intrusions.

The city enjoys a Mediterranean climate with mild winters and moderately hot summers. The prevailing wind regime in the zone during summer is the sea breeze, while the typical synoptic situations in winter have an Atlantic origin. The scarce annual precipitation, between 150 and 250 mm, is concentrated primarily in spring and fall, and the sparse ground vegetation in the region classifies the nearby surroundings as semi-arid. On dry and windy days these soil characteristics clearly enhance the levels of particles that arrive to the city, so a high contribution of resuspended soil dust is expected.

2.1. North African dust intrusion characteristics in the studied area

Southeast Spain is one of the areas along the western Mediterranean coast that receives particulate matter contributions with greater frequency due to its proximity to the African continent. In fact, approximately 16% of the air masses that arrive annually to the studied area have North African origins (Querol et al., 2008).

These outbreaks occur with the greatest frequency and intensity from spring to the beginning of fall. Moreover, during this period particle removal from the atmosphere is slower when compared to events produced in other periods of the year (Rodríguez et al., 2001). Events also occur during winter and early spring, although with a lower frequency. This type of transport is not common in November or December.

As a whole, between 16 and 19 episodes can take place annually, and elevated PM_{10} concentrations can be reached, but never exceed 150 $\mu g\,m^{-3}$ (Querol et al., 2004). The meteorological scenarios occurring under these episodes vary, depending upon the period of the year. These scenarios are described in Rodríguez et al., 2001.

3. Methodology

3.1. Sampling

PM_{10} samples were collected daily between December 2004 and November 2005, and 120 of them are analysed in this work. The selection criteria of the samples chosen for subsequent compositional analysis is based on achieving broad representativeness, both in the general processes and in the possible events, both anthropogenic and natural, that affect PM_{10} in the sampling area during the study period.

The 120 analysed samples (approximately one-third of the days during the study period) are representative of the occurrence of Saharan outbreaks, precipitation and any special events that occur during one entire year. In this way, approximately one-third of the outbreaks that took place in this period were analysed. Furthermore, to not produce skewed results the number of samples analysed per month was very similar.

The particulate matter samples were collected on 47 mm diameter quartz fibre filters by a low volume LVS.3.1 CEN EN 12341 reference sampler. The sampler was located at an urban background location, 12 m above ground level on a building roof. Total mass concentrations were obtained gravimetrically using an Ohaus AP250D microbalance (sensibility 10 μg), after conditioning the filters in a climate-controlled room at a temperature of 20 ± 1 °C and humidity of $50 \pm 5\%$.

3.2. Analytical techniques

The samples were analysed by Particle Induced X-ray Emission (PIXE) at the 3 MV Tandetron accelerator of the LABEC laboratory of the National Institute of Nuclear Physics (INFN) in Florence, Italy. An external beam facility fully dedicated to measuring elemental compositions of atmospheric aerosols has been installed there. Detailed

technical specifications of the setup and analysis conditions are reported in Calzolai et al. (2006). Here we will only briefly recall that thanks to the combined use of a Silicon Drift Detector (SDD), together with a traditional Si(Li) detector for the collection of low energy and high energy X-rays, respectively, it is possible to analyse quartz samples with measurements lasting only a few minutes ($\sim$5 min) to obtain elemental concentrations for all the elements with atomic number $Z > 10$. Due to the high silicon content in the filters themselves, it is not possible to measure the Si concentrations in the samples.

Since PIXE is a non-destructive technique, the same samples were additionally analysed by ion chromatography (IC) at the Laboratory of Atmospheric Pollution (LCA) of the Miguel Hernández University (Elche, Spain) to complete the sample composition. The ion chromatograph used is the DIONEX® model DX-120 with chemical autosuppression. An anionic column model AS9-HC and a cation column CS12A were used, both 250 mm in length and 4 mm in diameter. The ions determined in the samples were SO_4^{-2}, NO_3^- and NH_4^+.

For PIXE analysis, Minimum Detection Limits (MDL), at 1 σ level, are $\sim$10 ng m^{-3} for low-Z elements and $\sim$1 ng m^{-3} (or below) for medium- high Z elements, while the uncertainty of the elemental concentrations is in the range from 2 to 20%. For IC analysis the minimum detection limits were 0.01 μg m^{-3} (NH_4^+), 0.06 μg m^{-3} (NO_3^-) and 0.05 μg m^{-3} (SO_4^{-2}).

3.3. Detection of African dust outbreaks

Atmospheric dynamics and the detection of African dust outbreaks were performed by satellite images provided by the NASA SeaWifs project to detect dust plumes (McClain et al., 1998); two dust prediction models, the NAAPS model from the Naval Research Laboratory and the ICOD/DREAM model (Nickovic et al., 2001); back-trajectory calculation programs (HYSPLIT model, Draxler and Rolph, 2003), and NCEP meteorological maps (Kalnay et al., 1996). Meteorological data series from the Environmental Surveillance Network of the regional Government of Valencia were also used.

As an example, an episode identified as a Saharan dust outbreak, which occurred in the second fortnight of July 2005, is shown in Fig. 1. During this episode trajectories were found coming from south of Algeria and north of the Canary Islands. The SEAWIFS image confirmed the results of the ICOD and NAAPS models.

3.4. Data treatment: positive matrix factorization

The PMF model developed by Paatero and Tapper (1994) and Paatero (2004) is a method based on solving the factor analysis problem by least squares using a data point weighing method, which uses estimates of the data uncertainties to provide optimum data point scaling. A conventional factor analysis model can be written as

$$X = GF + E \tag{1}$$

where X is the known n x m matrix of the m measured elements or chemical species in n samples. G is an n x p matrix of source contributions to the samples (time variations). F is a p x m matrix of source compositions (source profiles). E is defined as a residual matrix, i.e., the difference between the measurement X and the model Y as a function of factors G and F.

$$e_{ij} = x_{ij} - y_{ij} = x_{ij} - \sum_{k=1}^{p} g_{ik} f_{kj} \tag{2}$$

Where $i = 1,\ldots, n$ samples; $j = 1,\ldots,m$ elements or chemical species; $k = 1,\ldots, p$ sources.

The PMF objective is to minimize the sum of the squares of the inversely weighed residuals with uncertainty estimates of the data points. Furthermore, PMF constrains all the elements of G and F to be non-negative, meaning that sources cannot have negative species concentration ($f_{kj} \geq 0$), and the sample cannot have a negative source contribution ($g_{ik} \geq 0$). The objective function to be minimized, $Q(E)$, is defined as

$$Q(E) = \sum_{i=1}^{m} \sum_{j=1}^{n} \left[\frac{e_{ij}}{s_{ij}}\right]^2 \tag{3}$$

where s_{ij} is an uncertainty estimate in the jth element measured in the ith sample. The solution of Eq. (3) is obtained by the PMF2 algorithm, in which both matrices G and F are adjusted in each iteration step. The process continues until convergence occurs (Paatero, 1997).

The Polissar et al. (1998) procedure was used to assign measured data and associated uncertainties as the PMF input data. The concentration values were used for the measured data and the sum of the analytical uncertainty, as well as one-third of the detection limit value was used as the overall uncertainty assigned to each measured value. Values below the detection limit were replaced by half of the detection limit values and their overall uncertainties were set at the sum of 1/2 of the average detection limits for this element and one-third of the detection limit values.

Since the chemical analysis was not sufficiently detailed (we are not sure that the unmeasured species can either be assumed to be strongly correlated to measured species or represent sources that add negligible mass to the particulate matter samples), the measured particulate matter mass concentration was included as an independent variable in the PMF model to directly obtain the mass apportionment without the usual multilinear regression. However, we performed also the analysis including the PM mass as dependent variable (with the MLRA). The results obtained were very similar to those obtained using the PM_{10} as an independent variable and no negative regression coefficients were obtained.

The estimated uncertainties of PM_{10} mass concentrations were set at four times their values so that the large uncertainties decreased their weight in the model fit. When the measured particulate matter mass concentration is used as a variable, the PMF apportions a mass concentration for each source according to its temporal variation. The PMF modelling results were normalized by the apportioned particulate matter mass concentration so that

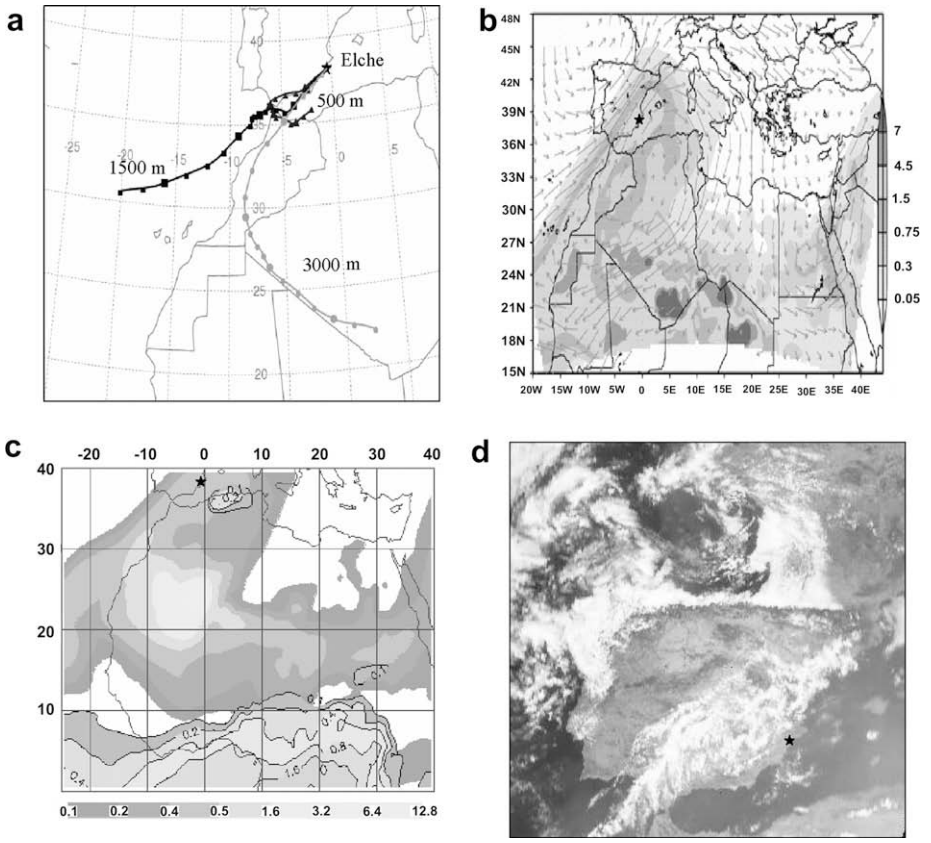

Fig. 1. Detection of a Saharan intrusion in Elche during the 17th of July 2005: (a) 4-d back-trajectories calculated by the HYSPLIT transport model (NOAA Air Resource Laboratory), at three different levels above the ground (500, 1500, and 3000 m), (b) dust loading forecast in the ICOD Model, (c) dust contribution in the NAAPS Optical Depth Model, (d) impact of Saharan dust illustrated by SEAWIFS satellite image.

the quantitative source contributions for each source were obtained. Specifically,

$$x_{ij} = \sum_{k=1}^{p} (c_k g_{ik}) \left(\frac{f_{kj}}{c_k} \right)$$

where c_k is the directly apportioned mass concentration by PMF for the kth source (Kim et al., 2004).

4. Results

4.1. PM_{10} levels and composition

Table 1 shows the mean PM_{10} concentrations obtained in each season during the study period. The standard deviations and absolute minimum and maximum values are reported as well.

Table 1
Mean value, PM_{10} daily maximum and minimum, and standard deviation (σ) in $\mu g\,m^{-3}$.

	PM_{10} ($n = 120$)	(σ)	Max.	Min.
Fall	26.1	(15.4)	66.2	9.3
Winter	37.3	(18.5)	73.8	12.1
Spring	30.9	(11.9)	55.1	12.1
Summer	39.6	(15.1)	73.5	14.2
Whole period	34.5	(16.2)	73.8	9.3

The annual average of PM_{10} mass concentration ($34.5\ \mu g\,m^{-3}$) lies within the range of values reported in literature for Spanish urban background sites, which is 30–46 $\mu g\,m^{-3}$ (Querol et al., 2008).

Table 2
Mean values, standard deviations, minima and maxima of the elemental and ionic concentrations ($ng\,m^{-3}$), and number of analysed samples ($n = 120$) with elemental concentration below the MDL.

Element/ion	Concentration	(σ)	Max.	Min.	# Samples <MDL
Na	979	(720)	3315	128	0
Mg	160	(101)	530	23	0
Al	520	(220)	1420	64	0
Cl	605	(509)	2270	60	0
K	288	(269)	5790	71	5
Ca	2174	(1115)	7090	270	0
Ti	32	(23)	410	6.2	1
V	12	(12)	89	2.3	14
Cr	3	(2)	10	1.1	29
Mn	7	(4)	21	2.2	1
Fe	341	(205)	1270	137	0
Ni	4	(3)	22	1.1	1
Cu	12	(9)	73	4.1	0
Zn	16	(12)	82	4.0	0
Br	5	(3)	16	1.3	1
Sr	8	(4)	82	1.0	0
Pb	6	(4)	31	0.4	17
SO_4^{-2}	4553	(3216)	17,200	687	0
NO_3^-	3705	(3040)	21,670	340	0
NH_4^+	1634	(1407)	6730	81	0

Table 3
Increment factors in elements and crustal ratios due to outbreaks.

	Outbreak day (n = 28)	Normal day (n = 42)	Increment factor
PM_{10}	50,675	27,803	1.82
Mg	176	95	1.85
Al	778	424	1.83
K	356	194	1.84
Ca	3138	1854	1.69
Ti	56	20	2.80
Mn	10	5	2.00
Fe	533	242	2.20
Sr	11	7	1.57
Ti/Ca	0.0181	0.0118	1.53
Ti/Fe	0.105	0.085	1.24
Al/Ca	0.251	0.253	0.99
Fe/Ca	0.170	0.140	1.22

Strong seasonal variations have been observed, with higher concentration values during summer and winter and lower values in fall (the average summer concentration is 13.5 $\mu g\,m^{-3}$ higher than the fall one). A statistical test (Student's-test with a 95% confidence interval) confirmed that spring-summer and fall-summer measurements are not "statistically" equal.

The higher concentrations measured during the summer months can be explained by the higher impact of local resuspension processes, the increase in the frequency and intensity of Saharan dust outbreaks, and the more intense photochemical activity. The high winter concentrations can be ascribed to an increase in vehicle and domestic heating use during the colder months. Traffic volume data, provided by the City Council, confirmed that the number of vehicles circulating within the City is about 30% higher in winter than in summer. Moreover, high pollution episodes occur with a certain frequency during situations of small mixing layer height and high meteorological stability, substantially increasing the mass concentrations. Lower PM_{10} concentrations have been measured in spring and fall, seasons characterized by a higher precipitation level. During the studied period, the seasonal accumulated precipitation was the following: winter (45.4 $l\,m^{-2}$), spring (26.1 $l\,m^{-2}$), summer (18.2 $l\,m^{-2}$) and fall (92.5 $l\,m^{-2}$). Although the intensity of the rain during spring was lower than during winter, the number of days with precipitation was higher in spring.

For all the analysed samples (120) the PM_{10} concentration exceeded the limit value established by European Directive 2008/50/CE on 25 occasions. A great percentage of these exceedances are due to events of natural origin, like Saharan episodes.

4.1.1. Elemental and ionic composition

Table 2 shows the mean concentrations along with the corresponding standard deviations, as well as the maximum and minimum ion and element values, which were analysed by IC and PIXE techniques. The number of analysed samples (n = 120) with elemental concentration below the MDL is also shown.

Some elements, like As, Se and Cd, were detected in a very low percentages of the samples, less than 20%, and hence they were not included in the study.

Mean values reported in Table 2 are similar to those recorded at other stations in the Iberian Peninsula with similar urban environments (Querol et al., 2008). The important contribution (close to 30%) of inorganic secondary compounds to the total PM_{10} mass stands out.

4.2. Signature of Saharan dust outbreaks

A total of 28 samples pertaining to nine Saharan outbreaks at the study area were analysed. The majority of them, 19, correspond to episodes occurring during spring and summer. During these events the PM_{10} limit value established by the European directive of 50 $\mu g\,m^{-3}$ was exceeded on 15 days. This provides an idea of the important contribution that these events have upon the total calculation of annual exceedances of this value. In this case, 60% of the total exceedances (25 days) occur during Saharan dust outbreaks.

Back-trajectory analysis and visualization of models and images determined that all the Saharan episodes originated in the western portion of the northern half of the African continent. This area spans central and southern Algeria, Morocco, northern Mali and Mauritania, in addition to Western Sahara.

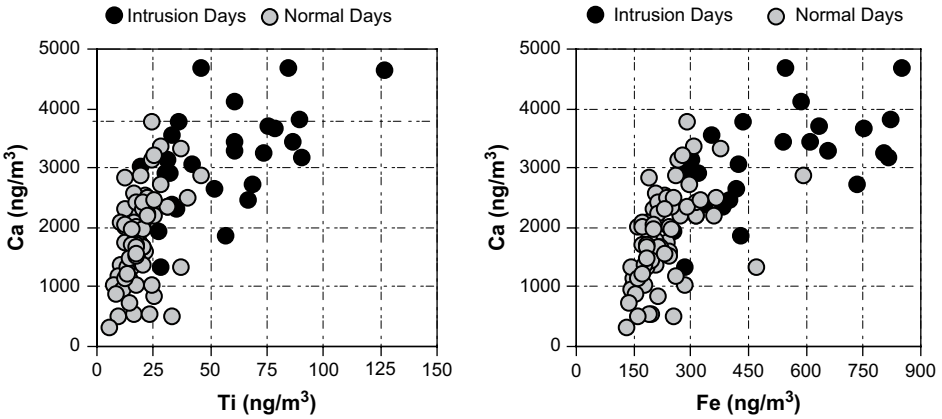

Fig. 2. Variation in the Ti/Ca and Fe/Ca ratio during intrusion periods and normal days.

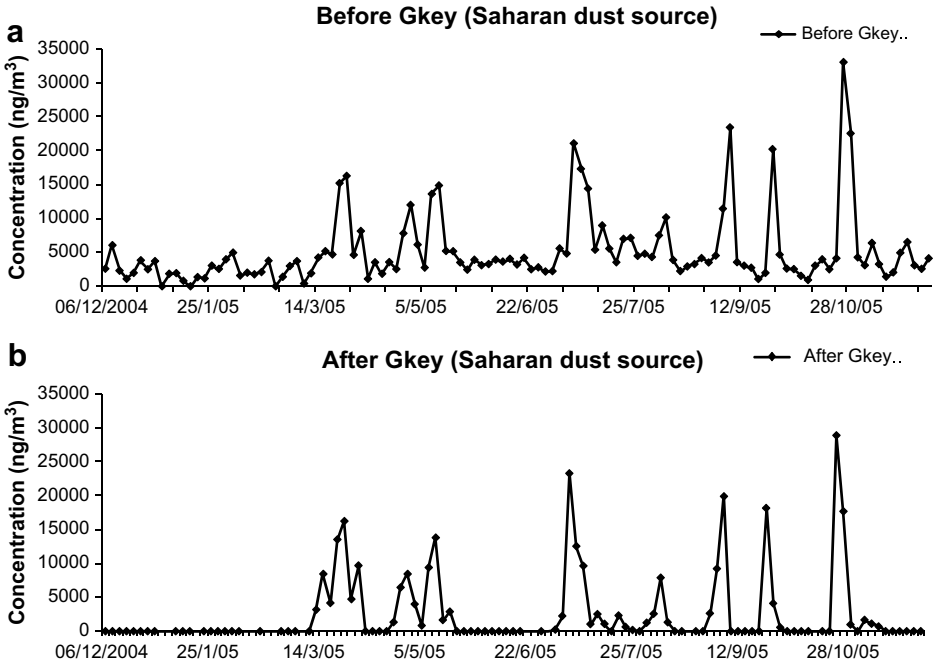

Fig. 3. Time pattern of the Saharan source identified by PMF: (a) without the use of the Gkey matrix, (b) with the use of the Gkey matrix (see explanations in the text).

The concentration increase due to these Saharan outbreaks did not affect equally all the crustal elements. Table 3 shows the increment factors for PM_{10} and for crustal elements concentrations during these episodes, with respect to values registered on normal days (i.e. those unaffected by either outbreaks or any other notable event, like intense rains or accumulation episodes). The concentrations are expressed in ng m^{-3}.

From the table it is evident how Ti is the element whose concentration increases the most during these events, nearly tripling. On the contrary, Ca and Sr show the smallest increase. Thus the Ti/Ca ratio is a good marker for these kinds of events in the study area. Its increment factor, 1.53, is very similar to that found by Borbély-Kiss et al. (2004), at an urban area in Hungary, or by Marenco et al. (2006), at the Global Atmospheric Watch Station of Monte Cimone (2165 m amsl), Italy. The Al/Ca ratio in these two cited studies presented a notable increase but showed no variation at our sampling site.

Fig. 2 shows the concentration of Ca versus the concentrations of Ti and Fe. As can be seen, the Ca/Ti and Ca/Fe ratios change significantly during most of the days identified as intrusion days, mostly when PM_{10} concentration is higher, that is when there is a strong dust deposition at the ground level; in some occasion we do not observe any effect because the outbreak has not a strong impact at ground level.

Table 4
Average source contributions (μg m^{-3}) to PM_{10} mass concentration.

	Average source contribution		
	Total average	Summer average	Winter average
Secondary nitrate	8.6	8.3	9.0
Secondary sulphate	7.6	10.1	4.3
Soil	7.1	8.1	5.9
Traffic	4.3	2.2	7.0
Sea	3.7	4.4	2.8
African dust	2.4	3.3	1.2

4.3. Positive matrix factorization

The goal of PMF analysis is to determine the number of sources and the corresponding profiles and contributions to PM mass.

In this work, PMF solutions for several choices of number of factors (from 3 to 9) and multiple values of FPEAK values were systematically explored (FPEAK values between −1 and +1 in steps of 0.2) and the resulting *Q*, IM, IS values, scaled residuals as well as *F* and *G* matrices were examined to find out the most reasonable solution. A 6 factor solution, with FPEAK = 0, resulted the best choice, in terms of both quality of the fit and physical sense for the studied system.

With the 5, 6 and 7 factor solutions and FPEAK = 0, the theoretical value *Q*, approximately equal to the number of degrees of freedom or number of input data points minus the number of the solution values, was approximately achieved. The only difference between the 5 sources solution and the 6 was that in the former the secondary nitrate and sulphate appeared in the same source (sometimes it happens because the SO_2 and NO_2 oxidation mechanism are very highly correlated), while in the 6 source solution we found these two sources were separated. With the 7 factor solution we obtained exactly the same sources found

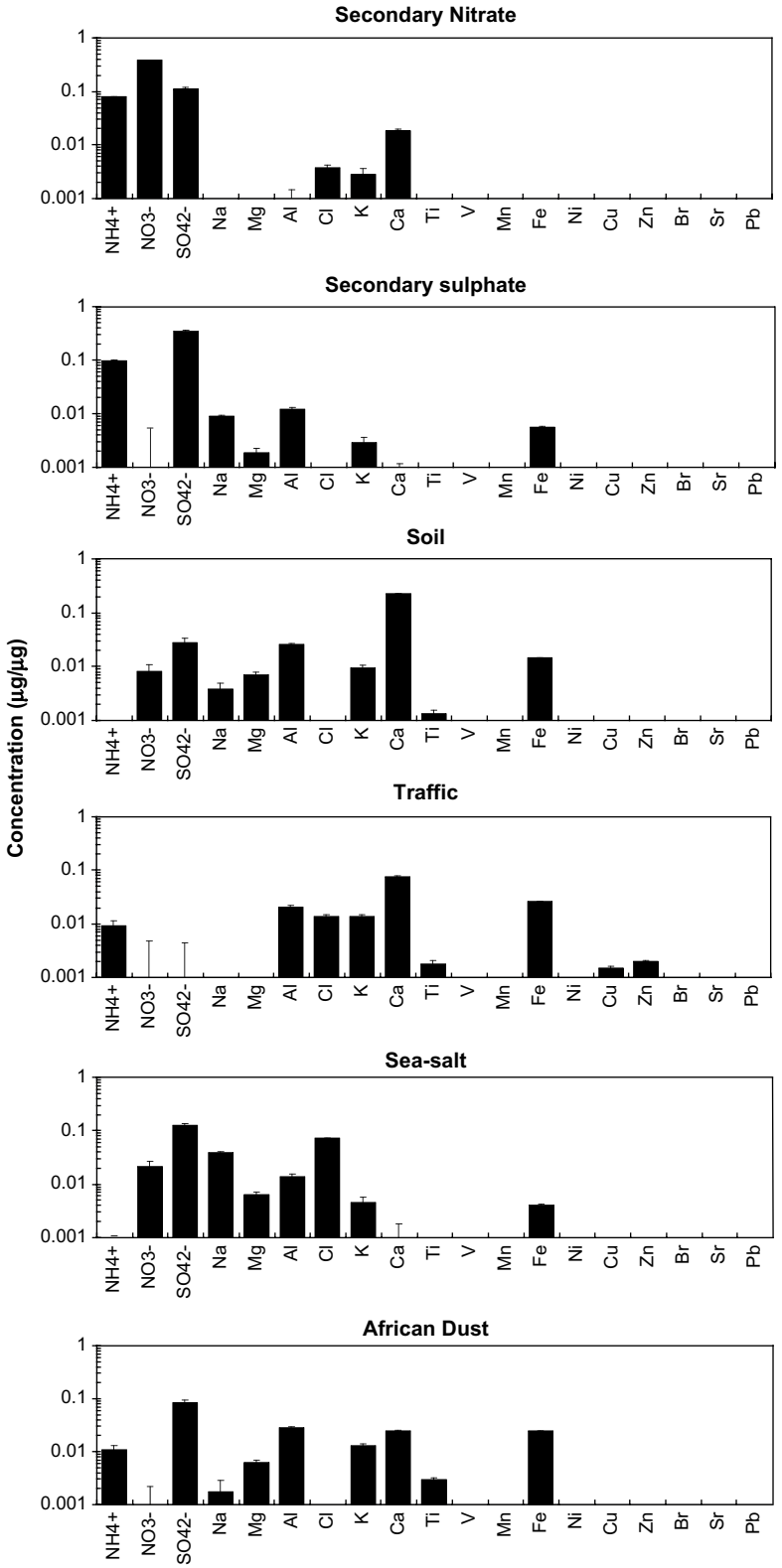

Fig. 4. Source profiles (prediction ± standard deviation) of the resolved sources measured at Elche.

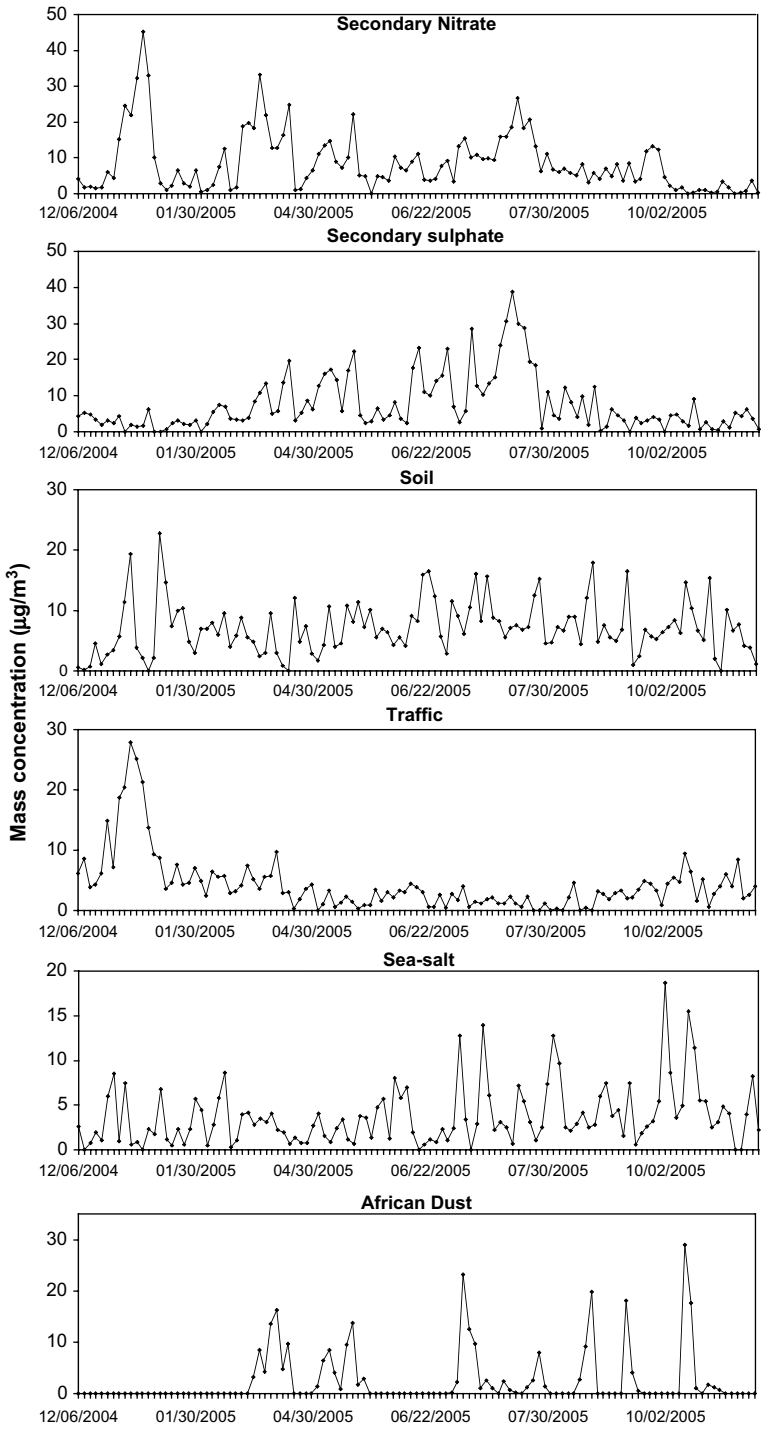

Fig. 5. Temporal variation of source contribution for the Elche site using the PMF model.

with the 6 one plus a source with a unique element without any characteristic time pattern. It was not clear what the origin of this source was. Then we selected the 6 factor solution.

Among the identified 6 sources, two of them are soil-like sources. One of these shows a high contribution during the 28 days we have already identified as intrusion days. Furthermore, its source profile is different from the one of the other soil source (for example, a higher contribution from Ti as expected for Saharan dust intrusion).

However, low but non-zero contributions on non-Saharan intrusion days were found, probably due to the

difficulty of distinguish Saharan dust from local dust sources. In order to quantify correctly the apportionment of the Saharan source to PM_{10} mass, we performed a refined PMF analysis. In PMF an external information can be imposed to the solution to control the rotations. If a certain source is inactive during certain days, it is then possible to pull the source contribution down toward zero through appropriate Gkey settings (Paatero, 2004; Song et al., 2006).

After several trials, the values in the Gkey matrix were set to 6 on non-Saharan days in order to achieve a negligible contribution. On the days with Saharan intrusions the Gkey values were set to the standard value (0).

In Fig. 3 the temporal pattern of the Saharan dust source obtained before and after Gkey application are reported. The use of the Gkey matrix did not introduce any significant difference for the other identified sources and for the Saharan dust source during the intrusion days.

Table 4 summarizes the six sources and their average mass contributions. A comparison of the PM_{10} mass contributions from all sources with measured PM_{10} mass concentrations yields good agreement ($r^2 = 0.92$). Figs. 4 and 5 illustrate the identified source profiles and time-series plots of daily contributions to PM_{10} mass concentration from each source, respectively.

The first source characterized by Al, Ca, Fe, K, and Sr has been identified as a "local soil" source. This may be the result of local and regional resuspension by wind and convective processes. Ca predominates due to the soil in the area being very rich in carbonates and calcium bicarbonates (the average Ca concentration is greater than 2 $\mu g\,m^{-3}$). The average contribution of this source is higher during summer (Table 4).

The "secondary nitrate" source is characterized by a high quantity of NO_3^-. The temporal evolution shows different maxima throughout the year. The higher concentrations were registered in winter during an accumulation period, while in summer high concentrations are due to the reaction of $HNO_3(g)$ with $CaCO_3$ or NaCl that results in forming larger sized calcium and sodium nitrate.

The "secondary sulphate" source is primarily formed by SO_4^{-2} and NH_4^+, indicating that the ammonium sulphate is the primary compound of this source. The seasonal evolution of this source is characterized by a clear maximum in summer due to greater SO_2 oxidation from high radiation and temperature levels reached during this time of the year in the study area.

"Traffic" is the fourth source, primarily characterized by the presence of Cu, Zn and some crustal elements. It correlates very well with Pb, whose concentration is so small that it is not visible in Fig. 4. The traffic factor is characterized by high levels in winter, while in summer it is reduced due to the rise of the mixing layer and a decrease in the number of vehicles during the summer holiday period. Note that the nitrate source (where a presence of elements like Cl, K, Pb can be observed) also receives contributions from traffic.

"Marine aerosol" is the fifth source, primarily characterized by the presence of Cl, Na and Mg. This source is also important due to the proximity to the sea. No seasonal evolution is observed, apart from several peaks that are dependent upon the wind direction.

Finally, the last source is again characterized by crustal elements (Al, Ti, Ca, Mg, Mn and Fe). Unlike the soil source, the greatest correlation of this source appears with Ti, a clear marker of the African transport episodes as explained above. If the temporal evolution is observed, marked peaks appear in coincidence with the predicted intrusions episodes as previously mentioned.

For what concerns annual averages, secondary nitrate was the major mass contributor on total average, accounting for 26% of the total PM_{10} mass. Secondary sulphate and traffic explained 22% and 13% of the bulk mass, respectively, while soil represented 21% and sea-salt 11%. African dust comprised another 7% of the PM_{10} mass.

4.3.1. *Importance of the African dust source*

The identification of the African dust source allows determining the contribution of Saharan episodes to the total PM_{10} mass. The contribution varies according to the intrusion days, within a range of 5–40% of the total PM_{10} mass concentration. On July 16, 2005, for example, the PM_{10} concentration was 58 $\mu g\,m^{-3}$; from the PMF analysis it was determined that the Saharan source contribution to the PM_{10} value was 24 $\mu g\,m^{-3}$, accounting for about 40% of the total mass.

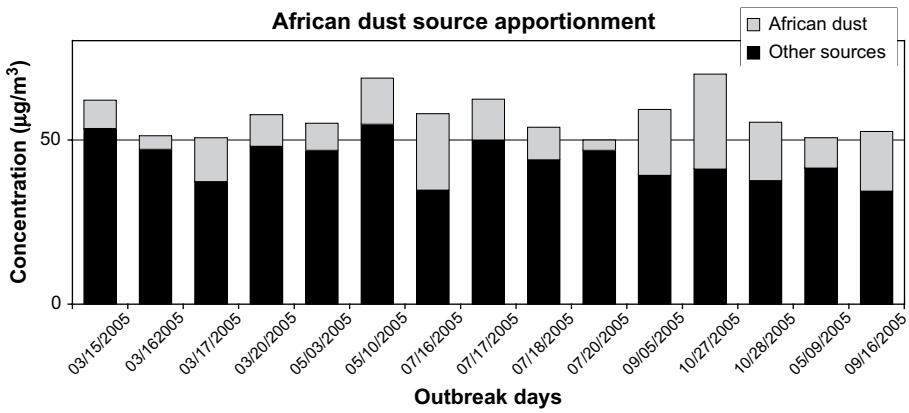

Fig. 6. African dust contribution for the days with a PM_{10} value greater than 50 $\mu g\,m^{-3}$.

This methodology can be applied to all intrusion days. Most of the outbreak days would no longer exceeded the threshold value of 50 $\mu g\,m^{-3}$ if the African dust source contribution was subtracted (Fig. 6). Only two days continue to exceed the 50 $\mu g\,m^{-3}$ threshold, due to appearance of sources other than the African dust one.

5. Conclusions

The first characterization of aerosol composition was achieved in Elche, a medium-size Spanish city, was achieved. This area is characterized by very low precipitation levels and thus could be considered an arid region. In addition, frequent Saharan intrusions reach the region due to its proximity to the African continent. The chemical composition of local and Saharan dust sources is very similar and therefore it is difficult to distinguish their contributions to PM_{10} mass concentration.

Positive matrix factorization identified six PM_{10} sources: ''local soil'', ''secondary nitrate'', ''secondary sulphate'', ''traffic'', ''marine aerosol'' and ''African dust''. Soil and African dust sources are both characterized by crustal elements, but the latter is mainly correlated with Ti, which resulted a clear marker of Saharan dust outbreaks, and peaks in its time pattern occur during intrusion episodes.

PMF was able to identify a Saharan dust source even in the presence of a strong local dust source, and the contribution of these two sources to PM_{10} over the study period was quantitatively estimated. The source contributions are respectively 21% and 7% of the PM_{10} mass over the study period. The African dust contribution varies according to the intrusion days, within a range of 5–40% of the total PM_{10} concentration.

Thanks to the separation between these two similar sources it is possible to subtract the African dust contribution from the daily PM_{10} mass concentration on days when it exceeds the 50 $\mu g\,m^{-3}$ limit value fixed by EU Directive 2008/50/CE. In this way it is possible to determine the number of exceedances which are not due to the Saharan contribution. The exceedances reduction is near 90% on the days influenced by Saharan dust intrusions and more than 50% of the total exceedances during the study period.

Acknowledgements

This work was supported by the Ministerio de Educación y Ciencia under the CGL2004-04419/CLI (RESUSPENSE) project. We would like also to thank Paul Nordstrom for his support.

References

Artiñano, B., Salvador, P., Alonso, D.G., Querol, X., Alastuey, A., 2003. Anthropogenic and natural influence on the PM_{10} and $PM_{2.5}$ aerosol in Madrid (Spain). Analysis of high concentration episodes. Environmental Pollution 125, 453–465.

Avila, A., Queralt, I., Alarcon, M., 1997. Mineralogical composition of African dust delivered by red rains over North-Eastern Spain. Journal of Geophysical Research 102, 21977–21996.

Bonelli, P., Marcazzan, G.M., Cereda, E., 1996. Elemental Composition and Air Trajectories of African Dust Transported in Northern Italy. Kluwer Academic Publishers. 275–283.

Borbély-Kiss, I., Kiss, A.Z., Koltay, E., SzabóGy., Bozó, L., 2004. Saharan dust episodes in Hungarian aerosol: elemental signatures and transport trajectories. Journal of Aerosol Science 35, 1205–1224.

Calzolai, G., Chiari, M., García Orellana, I., Lucarelli, F., Migliori, A., Nava, S., Taccetti, F., 2006. The new external beam facility for environmental studies at the Tandetron accelerator of LABEC. Nuclear Instruments and Methods in Physics Research Section B: Beam Interactions with Materials and Atoms 249 (1–2), 928–931.

D'Almeida, G.A., 1986. A model for Saharan dust transport. Journal of Climate and Applied Meteorology 25, 903–916.

Draxler, R.R., Rolph, G.D., 2003. HYSPLIT (Hybrid Single-Particle Lagrangian Integrated Trajectory). NOAA Air Resources Laboratory, Silver Spring, MD Model access via NOAA ARL READY Website. Available from: http://www.arl.noaa.gov/ready/hysplit4.html.

Dulac, F., Tanré, D., Bergametti, G., Buat-Ménard, P., Desbois, M., Sutton, D., 1992. Assesement of the African dust mass over the Western Mediterranean sea using Meteosat data. Journal of Geophysical Research 97, 2489–2506.

Guerzoni, S., Molinaroli, E., Chester, R., 1997. Saharan dust inputs to the western Mediterranean Sea: depositional patterns, geochemistry and sedimentological implications. Deep-Sea Research II 44 (3–4), 631–654.

Henry, R.C., Hidy, G.M., 1979. Multivariate analysis of particulate sulphate and other air quality variables by principal components - Part I. Annual data from Los Angeles and New York. Atmospheric Environment 13, 1581–1596.

Kalnay, E., Kanamitsu, M., Kistler, R., Collins, W., Deaven, D., Gandin, L., Iredell, M., Saha, S., White, G., Woollen, J., Zhu, Y., Leetmaa, A., Reynolds, B., Chelliah, M., Ebisuzaki, W., Higgins, W., Janowiak, J., Mo, K.C., Ropelewski, C., Wang, J., Jenne, R., Joseph, D., 1996. The NCEP/NCAR 40-year reanalysis project. Bulletin of the American Meteorological Society 77, 437–471.

Kim, E., Hopke, P.K., Edgerton, E.S., 2004. Improving source identification of Atlanta aerosol using temperature resolve carbon fractions in positive matrix factorization. Atmospheric Environment 38, 3349–3362.

Koçak, M., Kubilay, N., Mihalopoulos, N., 2004. Ionic composition of lower tropospheric aerosols at northeastern Mediterranean site: implications regarding sources and long-range transport. Atmospheric Environment 38, 2067–2077.

Kubilay, N., Nickovic, S., Moulin, C., Dulac, F., 2000. An illustration of the transport and deposition of mineral dust onto the eastern Mediterranean. Atmospheric Environment 34 (8), 1293–1303.

Marenco, F., Bonasoni, P., Calzolari, F., Ceriani, M., Chiari, M., Cristofanelli, P., ÁAlessandro, A., Fermo, P., Lucarelli, F., Mazzei, F., Nava, S., Piazzalunga, A., Prati, P., Valli, G., Vecchi, R., 2006. Characterization of atmospheric aerosols at Monte Cimone, Italy, during summer 2004: source apportionment and transport mechanisms. Journal of Geophysical Research 111, D24202. doi:10.1029/2006JD007145.

McClain, C.R., Cleave, M.L., Feldman, G.C., Gregg, W.W., Hooker, S.B., Kuring, N., 1998. Science quality SeaWiFS data for global biosphere research. Sea Technology 39, 10–16.

Nickovic, S., Papadopoulos, A., Kakaliagou, O., Kallos, G., 2001. Model for prediction of desert dust cycle in the atmosphere. Journal of Geophysical Research 106, 18113–18129.

Paatero, P., Tapper, U., 1994. Positive matrix factorization: a non-negative factor model with optimal utilization of error estimates of data values. Environmetrics 5, 111–126.

Paatero, P., 1997. Least squares formulation of robust non-negative factor analysis. Chemometrics and Intelligent Laboratory Systems 38, 223–242.

Paatero, P., 2004. User's guide for positive matrix factorization programs PMF2 and PMF3, Part. 1: tutorial.

Polissar, A.V., Hopke, P.K., Malm, W.C., Sisler, J.F., 1998. Atmospheric aerosol over Alaska-2. Elemental composition and sources. Journal of Geophysical Research 103 (D15), 19045–19057.

Querol, X., Alastuey, A., Rodríguez, S., Viana, M.M., Artiñano, B., Salvador, P., Garcia Dos Santos, S., Fernández- Patier, R., de La Rosa, J., Sánchez de la Campa, A., Menéndez, M., Gil, J.J., 2004. Levels of particulate matter in rural, urban and industrial sites in Spain. Science of the Total Environment 334–335, 359–376.

Querol, X., Alastuey, A., Moreno, T., Viana, M.M., Castillo, S., Pey, J., Rodríguez, S., Artiñano, B., Salvador, P., Sánchez, M., Garcia Dos Santos, S., Herce Garraleta, M.D., Fernandez- Patier, R., Moreno-Grau, S., Negral, L., Minguillon, M.C., Monfort, E., Sanz, M.J., Palomo-Marín, R., Pinilla-Gil, E., Cuevas, E., 2008. Spatial and temporal variations in airborne particulate matter (PM_{10} and $PM_{2.5}$) across Spain 1999–2005. Atmospheric Environment 42, 3964–3979.

Rodríguez, S., Querol, X., Alastuey, A., Kallos, G., Kakaliagou, O., 2001. Saharan dust contributions to PM_{10} and TSP levels in Southern and Eastern Spain. Atmospheric Environment 35, 2433–2447.

Ryall, D.B., Derwent, R.G., Manning, A.J., Redington, A.L., Corden, J., Millington, W., Simmonds, P.G., O'Doherty, S., Carslaw, N., Fuller, G.W., 2002. The origin of high particulate concentrations over the United Kingdom. Atmospheric Environment 36 (8), 1363–1378.

Salvador, P., Artiñano, B., Querol, X., Alastuey, A., Costoya, M., 2007. Characterisation of local and external contributions of atmospheric particulate matter at a background coastal site. Atmospheric Environment 41, 1–17.

Sánchez Gómez, M.L., Ramos Martín, M.C., 1987. Application of cluster analysis to identify sources of airborne particles. Atmospheric Environment 21 (7), 1521–1527.

Schwikowski, M., Seibert, P., Baltensperger, U., Gaggeler, H.W., 1995. A study of an outstanding Saharan dust event at the high-alpine site Jungfraujoch, Switzerland. Atmospheric Environment 29 (15), 1829–1842.

Song, Y., Zhang, Y., Xie, S., Zeng, L., Zheng, M., Salmon, L.G., Shao, M., Slanina, S., 2006. Source apportionment of PM2.5 in Beijing by positive matrix factorization. Atmospheric Environment 40, 1526–1537.